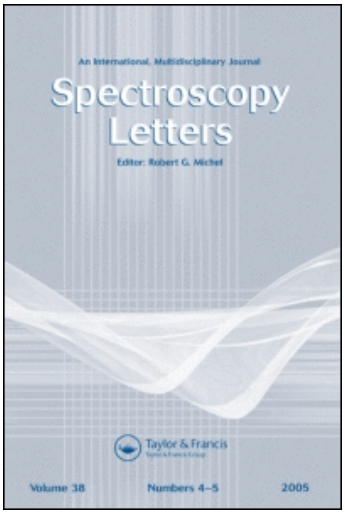

Spectroscopy Letters
Publication details, including instructions for authors and subscription information:
http://www.informaworld.com/smpp/title~content=t713597299

On the Thermal Decomposition of Dipyridamole: Thermogravimetric, Differential Scanning Calorimetric and Spectroscopic Studies

Marilene Silva Oliveira[a]; Sylvana Cardoso Miguel Agustinho[a]; Ana Maria de Guzzi Plepis[a]; Marcel Tabak[a]
[a] Instituto de Química de São Carlos, Universidade de São Paulo, São Carlos, SP, Brazil

To cite this Article Oliveira, Marilene Silva , Agustinho, Sylvana Cardoso Miguel , Plepis, Ana Maria de Guzzi and Tabak, Marcel(2006) 'On the Thermal Decomposition of Dipyridamole: Thermogravimetric, Differential Scanning Calorimetric and Spectroscopic Studies', Spectroscopy Letters, 39: 2, 145 — 161
To link to this Article: DOI: 10.1080/00387010500531126
URL: http://dx.doi.org/10.1080/00387010500531126

Spectroscopy Letters, 39: 145–161, 2006

ISSN 0038-7010 print/1532-2289 online
DOI: 10.1080/00387010500531126

On the Thermal Decomposition of Dipyridamole: Thermogravimetric, Differential Scanning Calorimetric and Spectroscopic Studies

Marilene Silva Oliveira, Sylvana Cardoso Miguel Agustinho, Ana Maria de Guzzi Plepis, and Marcel Tabak
Instituto de Química de São Carlos, Universidade de São Paulo, São Carlos, SP, Brazil

Abstract: Thermal decomposition of dipyridamole was followed by analysis of the residue by spectroscopic methods. The loss of mass observed in thermogravimetric (TG) experiments in N_2 atmosphere occurs in essentially three steps. The first step, corresponding to 35% of mass loss, was monitored in an isothermal process, and the solid residue was analyzed by proton and carbon NMR, optical absorption, and fluorescence emission. Heating at 305°C leads to new products with optical absorption bands shifted to lower wavelengths relative to dipyridamole. The broad emission band is also shifted to lower wavelengths. NMR analysis demonstrates that the piperidine groups are probably one of the sites of modification because the corresponding resonance peaks are not present in proton or carbon spectra. Preliminary high-pressure chromatography shows that two main compounds appear at significantly higher polarity as compared with dipyridamole. Isothermal decomposition leaves the pyrimido-pyrimidine central ring essentially unchanged, and the products involve changes at the peripheral substituent positions. Our results further contribute to elucidate the chemistry of this class of compounds.

Keywords: Dipyridamole, DSC, fluorescence emission spectroscopy, IR, NMR spectroscopy, optical absorption spectroscopy, thermal decomposition, TG

Received 7 March 2005, Accepted 29 August 2005
Address correspondence to Marcel Tabak, Instituto de Química de São Carlos, Universidade de São Paulo, São Carlos SP, Brazil. E-mail: marcel@sc.usp.br

INTRODUCTION

Dipyridamole (DIP), 2,6-bis-[bis-(2-hydroxyethyl)-amino]-4,8-dipiperidino-pyrimido[5,4-d]-pyrimidine, is a drug used in cardiovascular diseases due to its vasodilating and antiplatelet properties.[1,2] Research from many laboratories in recent years has shown that besides the mentioned properties and its use for treatment of angina pectoris and myocardial infarction, DIP has also an antioxidant effect in membrane systems and a coactivator activity for tumor cells in the presence of antitumor chemical agents.[3–6] In particular, Iuliano et al.[7] have suggested that the antioxidant activity of dipyridamole is mainly due to the scavenging of peroxyl radicals. The classical antioxidant mechanism of phenols or amines involves the transfer of hydrogen atoms to peroxyl radicals. Pedulli et al.[8] suggested an alternative antioxidant mechanism for DIP that involves the transfer of electron to peroxyl radicals. Its structure, as shown in Fig. 1, presents a stable heteroaromatic pyrimido-pyrimidine ring core that is responsible for the characteristic electronic absorption and fluorescence emission bands.[9–11] Although this compound has been used for many years, its mechanism of action is still not known. Research in our laboratory has provided a considerable amount of data regarding the properties of DIP. In recent years, we have studied the electrochemical properties of DIP aiming to obtain more information, which could be useful to explain the antioxidant activity.[12,13] Electrochemical oxidation leads to extensive changes in the molecular structure of DIP giving several products with very different spectroscopic properties as compared with the original compound. For instance, the intrinsic intense fluorescence emission observed for DIP is totally abolished by the electrochemical oxidation. The characterization of these products and the determination of their chemical structure remains a matter for research, and the elucidation of this question

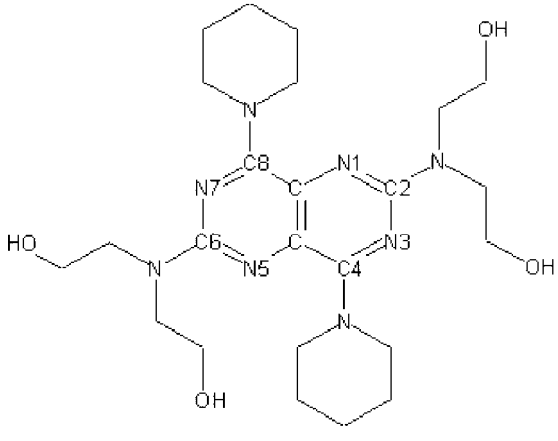

Figure 1. Structure of dipyridamole.

will contribute to a deeper understanding of the chemistry of this class of compounds. In the current work, a study with thermal techniques is presented with the aim to contribute further to the understanding of thermal stability of the compound and the characterization of the products of thermal decomposition, by means of thermogravimetric (TG) and differential scanning calorimetry (DSC) techniques, followed by the characterization of the products through UV-Vis absorption, fluorescence emission, and proton and carbon NMR spectroscopies. Recently, Berbenni et al.[14] have reported an interesting study on the thermoanalytical characterization of solid-state dipyridamole. They reported thermal transitions associated with different polymorphic crystal forms, which were discussed previously in Ref. [15] In the current work, the solid residue remaining after the thermal decomposition of DIP is solubilized in order to monitor the products obtained by heat treatment.

Preliminary HPLC experiments to obtain the products in their pure form in order to characterize them are also reported. An important observation in the current study is the retention of fluorescence by the products of thermal decomposition implying a less extensive structural change as compared with electrochemical oxidation.

EXPERIMENTAL

Dipyridamole was acquired from Sigma Chemical Co. (St. Louis, MO, USA) in powder form and used without further purification. TG and DSC curves were obtained using thermal analysis (TA) instruments (TA Instruments, USA): TG model 2050 and DSC model 2010, respectively. During the experiments, a heating rate of $10^{\circ}C\,min^{-1}$ was used, either in N_2 or synthetic air dynamic atmosphere, with a flux of $60\,mL\,min^{-1}$ for DSC and $90\,mL\,min^{-1}$ for TG. The sample pans were from platinum for TG and from aluminum, non-hermetic, for DSC. Sample weights were in the range of 5 to 25 mg. The measurements of UV-Vis and fluorescence emission were obtained using a UV-1601PC (Shimadzu, Japan) spectrophotometer in the range 250–600 nm, and a model F-4500 (Hitachi, Japan) spectrofluorimeter in the range 425–600 nm, respectively. Infrared spectra were measured in KBr pellets, and a FT-IR spectrometer model MB-102 (Bomen, Canada) was used. The NMR spectra were obtained using a model AC 200 (4.7 Tesla, Brucker, Germany) operating at 200.1 MHz for proton and 50.32 MHz for carbon-13. The preliminary chromatographic HPLC analyses were performed on a model Cromal HPLC (Shimadzu, Japan) equipped with 2 LC-10AD pumps, detector SPD-M10AVP UV-Vis detector, controlled for communication by Bus Module-CBM-10A. A model Luna C-18 (5 μm, 250 × 4.6 mm, Phenomenex Inc., USA) column was used, with a mobile phase consisting of a mixture acetate buffer 40 mM pH 4.0/MeOH. Chromatography was performed in isocratic and gradient modes, with a flux at $1\,mL\,min^{-1}$. Sample injection volume was 20 μL.

Isothermal experiments were performed in the following way: the balance was heated up to 305°C, followed by sample insertion, and maintaining it at this temperature for approximately 15 min. This time was sufficient for a reduction in sample mass from the initial value to the second plateau observed in TG experiments. The residual mass was dissolved in deuterated solvent (D_2O or DMSO-d_6) to perform NMR analysis. Optical spectroscopic (absorption and fluorescence emission) analysis and HPLC experiments were performed with these solutions as a stock by appropriate dilutions.

Additional DSC experiments were performed by heating, at the same rates mentioned above in a N_2 atmosphere, a DIP solid sample to either 150°C (before fusion) or 190°C (after fusion) temperatures, keeping the samples at these final heating temperatures for 15 min, followed by either a rapid or slow cooling, and performing a second heating cycle. The goal of this experiment was to monitor the reversibility of DIP fusion and the eventual existence of additional processes (besides the fusion) upon heating the compound up to a temperature above and below its fusion.

Electrooxidation of DIP in acetonitrile was performed for a 0.5 mM DIP solution prepared in the presence of 0.1 M lithium perchlorate as supporting electrolyte. This oxidation process is characterized by two oxidation waves (centered at potentials of + 340 and + 650 mV).[12,16] Controlled potential electrolysis was made at the second wave (E = +650 mV), and the products were monitored by optical absorption and fluorescence emission spectroscopies.[12,19]

Controlled potential electrolysis (CPE) experiments were conducted with a potentiostat/galvanostat EG&G-PAR model 273, using a three-compartment cell equipped with a 4.2 cm^2 area platinum foil working electrode in a mechanically agitated solution. After electrolysis, appropriate aliquots were taken from the sample cell to carry out the spectroscopic measurements, and control ultramicroelectrode (UME) voltammetric experiments were made to observe the characteristics of the oxidation products. The cation radical of DIP presented a relatively slow decay, which could be monitored by optical absorption spectroscopy.[12,16]

RESULTS AND DISCUSSION

Thermal Analysis

In Fig. 2, DSC curves of DIP in N_2 and synthetic air atmospheres are shown. A narrow endothermic transition at $T_p = 167.5$°C, associated with the melting of DIP, is observed. According to the literature,[17] the melting temperature of DIP is $T_f = 163$°C. In Ref.[14], the authors suggest that the fusion of solid DIP occurs in the range 163–168°C, after the transition between two polymorphic forms around 130°C, showing a peak in DSC curve ($T_p = 165.7$°C) consistent with this result. This is very similar to our observation. The value of ΔH of melting for the DIP was estimated from this

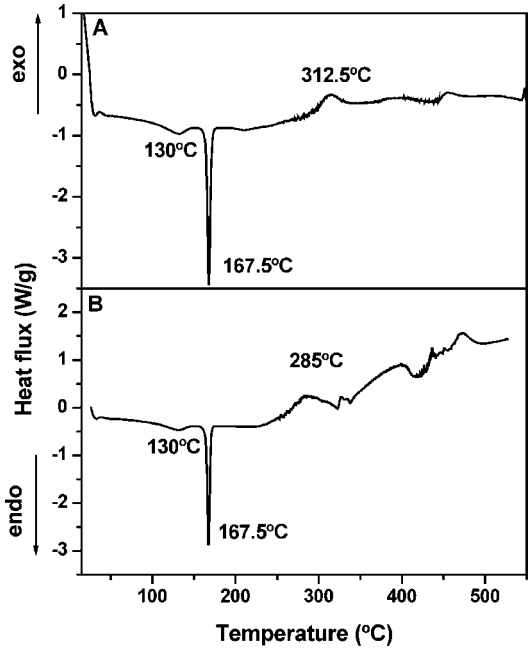

Figure 2. Dipyridamole DSC curves: (A) nitrogen atmosphere, (B) air atmosphere. Heating rate of 10°C min^{-1}. The sample weight was around 10 mg.

experiment as 36.3 kJ/mol and 30.7 kJ/mol, respectively, in N_2 and air atmospheres. Another transition, not so sharp and well defined, is also observed at higher temperatures and can be related to the decomposition of the compound. In the presence of air, the decomposition starts at 230°C having a peak at a temperature of 285°C (Fig. 2B), while in the presence of N_2 decomposition starts at 250°C having its peak at 312.5°C (Fig. 2A).

In Fig. 3, DSC curves obtained in an experiment where the solid sample was initially heated up to 190°C in N_2 atmosphere at a rate of 10°C min^{-1}, kept for 15 min at this temperature, followed by a slow cooling to ambient temperature (25°C) and a second heating cycle are presented. Two observations can be made: because the final heating temperature is higher than the fusion temperature, this experiment involves fusion, recrystallization, and a second fusion cycle. So, the first observation is the lowering of the fusion temperature in the second heating cycle to 160.6°C. The value of ΔH of melting is around 35% lower as compared with that in the first heating cycle as reported above. The second observation is that the broad transition observed before the first fusion cycle, and originally at around 130°C, has disappeared while a new weak transition around 65.6°C is observed (shown in inset to Fig. 3). The transition around 130°C was previously observed in Ref.[14] where it was associated with the existence of a hydrogen bond

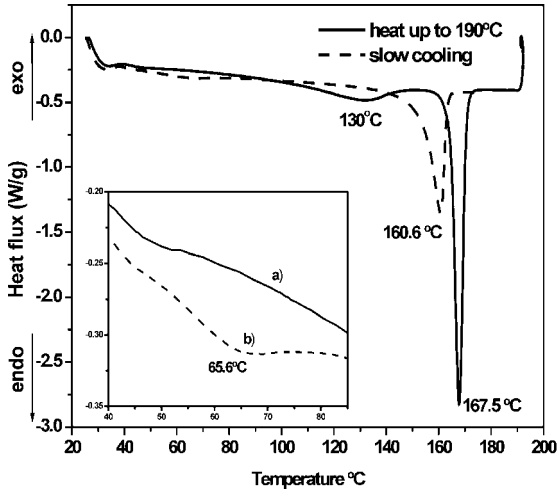

Figure 3. Dipyridamole DSC curves corresponding to a heating experiment up to 190°C in N_2 atmosphere (—), followed by a slow cooling to ambient temperature (25°C), and a second heating cycle (– – –). The inset shows the expanded low-temperature region underlaying the transition at 65.6°C. (a) heating up to 190°C and (b) slow cooling followed by a second heating cycle.

network in DIP crystalline state, and which was also described in the crystal structure determination.[15] The transition observed at 65.6°C presents a 10-fold decrease of the transition ΔH as compared with that at 130°C, implying that they could be of a different nature. Interestingly, if the cooling is rapid, the DSC curves are the same as in Fig. 3 with the absence of the transition at 65.6°C. It is also interesting that exposing solid DIP to milling for a time greater than 30 min completely abolishes the transition at 130°C.[14] A similar experiment where the solid sample was initially heated up to 150°C, kept for 15 min at this temperature, followed by a slow cooling to room temperature (25°C) and a second heating cycle has given a temperature shift of the transition from 130°C to 126°C together with a 20% reduction of transition ΔH. This effect is consistent with the findings in Ref.[14] where long exposures of solid DIP to 150°C lead to the lowering of its transition ΔH by a similar amount. In summary, the transition at 130°C associated with the hydrogen bond network in the solid DIP is abolished after exposure to temperatures higher than the fusion one, while it remains to a significant extent if the thermal treatment is performed below the fusion temperature. The possibility that this transition involves some water molecules strongly bound in the solid sample as reported for sugar derivatives, which have intrinsic bound water,[18] is ruled out from the fact that no changes (mass losses) are observed in TG-DTG curves (Fig. 4), in the temperature range from 30°C up to 200°C.

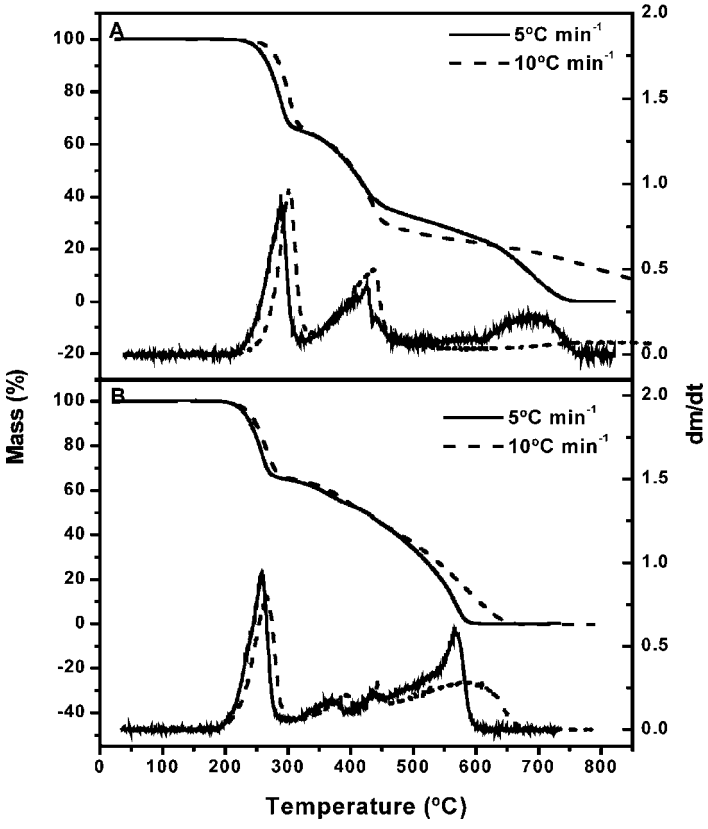

Figure 4. Dipyridamole TG-DTG curves: (A) nitrogen atmosphere, (B) air atmosphere. Heating rate of 5°C min^{-1} and 10°C min^{-1}. The sample weight was around 10 mg.

The loss of mass observed by TG experiments (Fig. 4) occurs essentially in three steps: an initial loss of 35% in the range of temperature 200–340°C (DTG peak at 300°C), followed by a second loss of 35% in the range 340–485°C (DTG peak at 430°C), and a final loss spread over higher temperatures. It is worth mentioning that, as the temperature increases above 240°C, some volatile product with an intense smell is produced. Attempts to trap this gaseous component for further analysis were not successful. The results presented above were obtained in an inert atmosphere of N_2 (Fig. 4A). The initial 35% loss of mass of DIP (M.W. 504 Da) corresponds to 176 Da, which, as will be shown later on, is probably associated with the dissociation of the two piperidine substituent groups (total mass of 168 Da) attached to carbons C4 and C8 of pyrimido-pyrimidine ring. The second loss of another 35% could be associated with the dissociation of the two diethanolic groups attached to the substituents at positions C2 and C6 of the central ring. If this is true, the pyrimido-pyrimidine central ring of DIP molecule is quite

stable even at relatively high temperatures. In an atmosphere saturated with oxygen, the TG-DTG curve changes slightly, as shown in Fig. 4B, particularly for the higher temperature processes, and the initial loss of mass seems to occur at a lower temperature as compared with the heating at nitrogen atmosphere; this observation can be related to the fact that DIP has a higher thermal stability in N_2 than in air. The loss of mass observed in the experiment of TG in atmosphere of air (Fig. 4B) occurs essentially in four steps: a loss of 35% in the range of temperature 180–310°C (DTG peak at 265°C), a second loss of 14% in the range 310–420°C (DTG peak at 392°C), a third loss of 7.5% in the range 420–460°C (DTG peak at 442°C), and a fourth loss of 43% at higher temperatures with DTG maximum at 587°C. These differences in the TG curve can be due to the reactions of the compound with the atmosphere, and especially in the presence of oxygen in the air, DIP could undergo oxidation at high temperature, a reaction that is not observed in inert atmosphere. Because DIP is a very efficient antioxidant,[7,8,19] it is not surprising that it is easily oxidized in the presence of air. Experiments at different heating rates were also performed: for a lower heating rate of $5\,^{\circ}C\,min^{-1}$ (Fig. 4) the decomposition occurs, as expected, at lower temperatures, therefore the process is slower, and the decomposition in the third and fourth steps of the curves in N_2 and air are more defined, respectively.

Optical Spectroscopy Studies

An isothermal experiment was performed to monitor in more detail the first loss of mass at 305°C in N_2 atmosphere. The products of isothermal decomposition (solid residue), monitored in the first step of decomposition (305°C), present a first fraction well-soluble in water and a second fraction that precipitates in water and is soluble in DMSO and was not analyzed in detail. In Fig. 5, the optical absorption and fluorescence emission spectra of DIP and of the products of isothermal decomposition soluble in aqueous solution are shown. Optical absorption spectrum of DIP is characterized by two bands, centered at 400 nm and 290 nm, respectively (Fig. 5A). Besides that, a strong fluorescence emission with maximum around 500 nm is observed upon excitation at 400 nm (Fig. 5B), in agreement with previous results.[9–11] The isothermal heating at 305°C leads to new products with absorption and emission bands shifted to lower wavelengths. The absorption spectrum showed two bands at 370 nm and 275 nm, and an intense fluorescence emission with maximum at 460 nm. The absorption and emission spectra for the fraction soluble in DMSO (data not shown) presented similar shifts to lower wavelengths with subtle differences as compared with the aqueous fraction. Electrochemical oxidation of DIP has been studied in detail in Ref.[16] Oxidation takes place in two sequential one-electron steps. Upon electrochemical oxidation in the second wave potential (+650 mV), the fluorescence of DIP (Fig. 6B) disappears completely and the absorption bands change dramatically with disappearance of

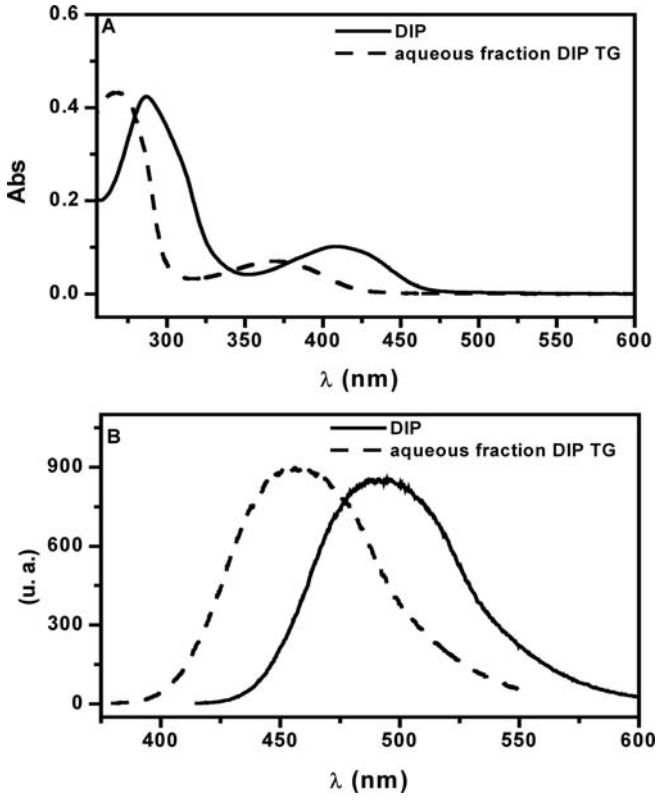

Figure 5. (A) Optical absorption spectra and (B) fluorescence emission spectra of pure original DIP (—) and of aqueous fraction of products of isothermal decomposition (– –). All spectra obtained as diluted samples in aqueous solvent, using quartz cuvettes of 1 cm optical length.

the visible band at 400 nm (Fig. 6A), suggesting extensive reorganization of the pyrimido-pyrimidine ring.[12,16] The absorption spectra in Fig. 6A show some time evolution after the electrolysis that is associated with chemical reactions that take place after the electrochemical oxidation, in particular to formation and decomposition of the cation radical of dipyridamole. This phenomenom is described in detail in Ref.[16] The spectroscopic results for the thermal decomposition products suggest smaller modifications of the structure of original DIP with the possiblity of mantainence of part of the heteroaromatic central ring, responsible for the fluorescence emission.

IR Study

In Fig. 7, the infrared spectra are presented for original DIP and the aqueous fraction obtained from the residual mass after the isothermal heating at

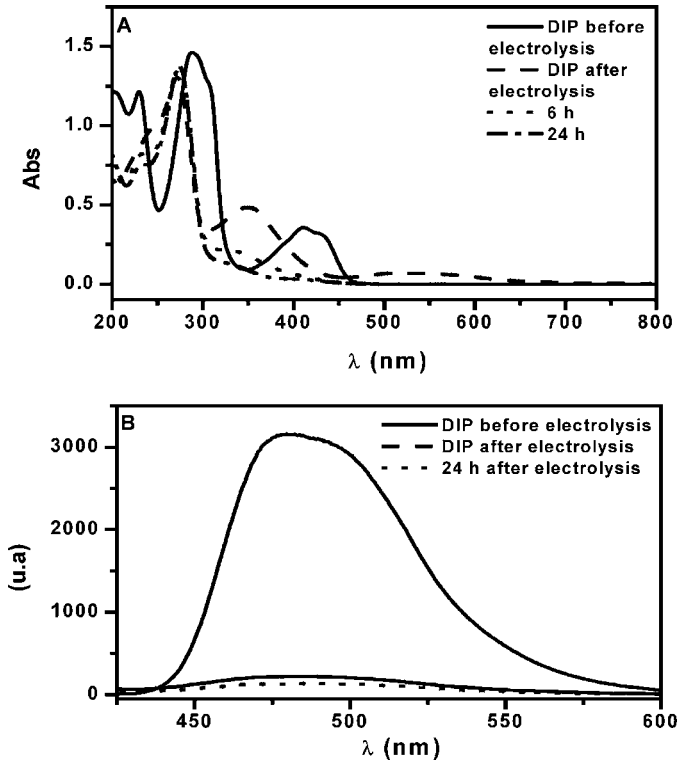

Figure 6. Optical absorption spectra of DIP 0.5 mM in acetonitrile (A) from an electrolysis experiment performed at a potential of +650 mV (two-electron oxidation) for 30 min. Spectra are presented before electrolysis, immediately after electrolysis, and after 6 hr and 24 hr after electrolysis. Fluorescence emission spectra (B) for the same DIP sample as in (A) showing drastic reduction of emission, using quartz cuvettes of 1 mm optical length.

305°C. The residue from the sample exposed to heating was dissolved in water, the soluble material was lyophilized, and a small fraction of solid material was used to produce the KBr pellet. In Table 1, the IR frequencies are shown corresponding to the main peaks in the IR spectra of Fig. 7. The main changes in the product IR spectrum as compared with original DIP [10,11,14,20] are seen as a shoulder in the region of 3300 cm^{-1}, which appears in the aqueous fraction and is absent in DIP; in the range 1800–1500 cm^{-1} where a broad band is observed for the aqueous fraction and is absent for DIP and the peak at 1292 cm^{-1} observed for the aqueous fraction and absent in DIP. The relatively broad band that spans the range from 1670 to 1582 cm^{-1} could be associated with the formation of a carbonyl group in the final product(s). This frequency range is usual for carbonyls in quinone derivatives.[21] Because a considerable amount of

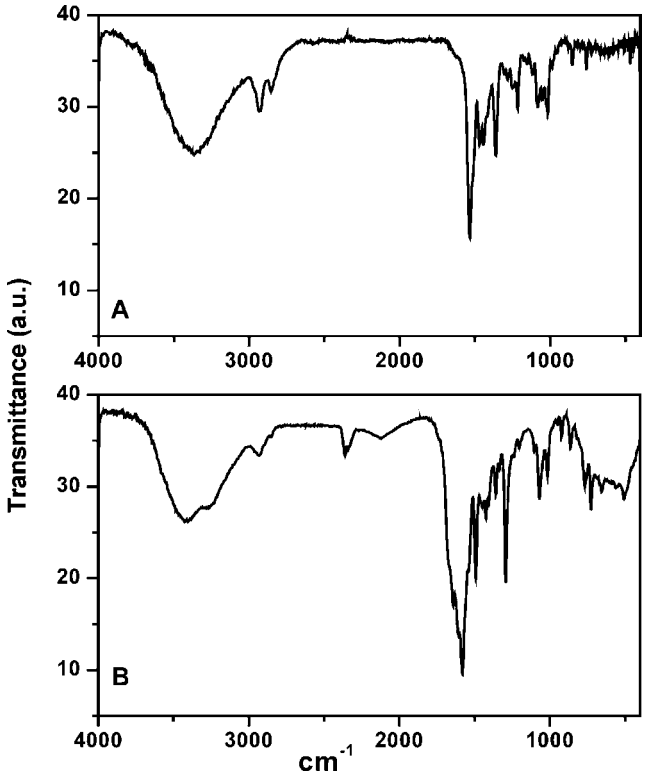

Figure 7. (A) Infrared spectra of DIP and (B) aqueous fraction obtained from the residue of isothermal experiment at 305°C in a KBr pellet.

aromaticity is retained in the products of isothermal decomposition of DIP at 305°C, the formation of this group could be considered.

NMR Analysis

In Fig. 8, the ^{1}H-NHR and ^{13}C-NMR spectra of the original DIP in D_2O are presented.[11,20,22] The spectrum of ^{1}H (Fig. 8a) presents the peaks of the CH_2 groups of the piperidine ring around 1.5 ppm, and the peaks of the CH_2 group neighbors of oxygen and nitrogen in the region between 3.4 ppm and 3.8 ppm. The NMR spectrum of ^{13}C (Fig. 8b) presents the peaks of the aromatic carbons in the range of 128 ppm and 160 ppm, the carbons of the CH_2 groups of the piperidine ring between 26 ppm and 29 ppm, and the carbons of the CH_2 group neighbors of oxygen and nitrogen between 52 ppm and 63 ppm.[20,22]

The ^{1}H-NMR spectrum from the D_2O fraction of the products of isothermal decomposition (Fig. 9a) show that the position of the corresponding peaks

Table 1. Infrared bands obtained for the aqueous fraction of DIP submitted to isothermal heating at 305°C as compared with original DIP

IR Frequency (cm^{-1})		
DIP	Aqueous fraction	Assignment
3361	3423	νOH
	3280^{sh}	
2932	2936	$\nu_{as}CH_2$
2851	2848^{sh}	ν_sCH_2
	$1670^{sh}-1642$	$\nu_sC{=}O$
	1607	
	1582	
1534	1538	$\nu C{=}N$ (ring)
1469	1493	δ_sCH_2
1444	1424	δ_sCH_2
1360	1357	$\nu C-N$
1217–1251	1292	
1083–1049	$1103^{sh}-1069$	$\nu_{as}(C-C-O)$
1016	1016	
	921	
853	863	
758	768	
	726	

The assignments for DIP IR frequencies are based on Refs.[10,11,14,16]

Superscript sh means the band is observed as a shoulder. DIP, dipyridamole.

of the methylene groups is considerably different from the spectrum of the original DIP, presented in the Fig. 8a: the peak of the carbon corresponding to the piperidine ring is practically absent from the spectrum of the carbon of the D_2O fraction (Fig. 9b). The presence of the aromatic ^{13}C peaks suggests also the maintenance of the electronic structure of the pyrimido-pyrimidine ring. This is consistent with the dissociation of the piperidines suggested as the initial step of mass loss in the TG-DTG experiment (Fig. 4) and retention of significant fluorescence emission by the products of thermal decomposition.

Preliminary Chromatographic Analysis

Thin-layer chromatography experiments with the aqueous fraction showed the existence of three spots with different polarity (data not shown), higher than that of the original DIP. This was confirmed by the preliminary HPLC analysis. Figure 10A shows the chromatogram from the aqueous fraction in

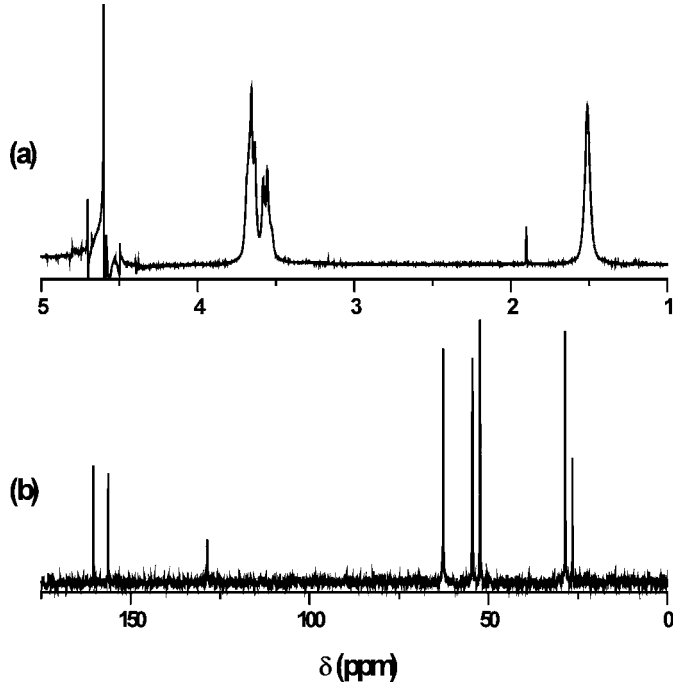

Figure 8. (a) ^{1}H-NMR and (b) ^{13}C-NMR spectra of DIP in D_2O in acid.

the gradient mode, using the mixture acetate buffer 40 mM pH 4.0/MeOH as mobile phase. The initial peaks of small intensity (peaks 1–4, Fig. 10A) were collected together forming one fraction F_{aq}I. The major peaks (peaks 5 and 6, Fig. 10A) were also collected, separately, forming the fractions F_{aq}II and F_{aq}III, respectively. These fractions were eluted at 10% MeOH in the initial 40 min of elution. The remaining peaks of the less polar compounds (peaks 7–12, Fig. 10A) were also collected together forming a fourth fraction F_{aq}IV. This fraction corresponds to material eluted at higher methanol content of mobile phase in the second step of the applied gradient. The major peaks for the aqueous fraction, peaks 5 and 6 in Fig. 10A, have retention times of 28.5 and 33.0 min, respectively, and correspond to 38.5% and 44.6% of the total material eluted from the column.

So, these two major fractions correspond to more than 80% of the total material. The characterization of these major peaks obtained in the preliminary HPLC experiments described above is presently being performed through spectroscopic methods. The chromatogram for pure DIP (Fig. 10B) in the isocratic mode in the mixture acetate buffer 40 mM pH 4.0/MeOH (3:7) showed a retention time of 10.5 min for DIP. Because DIP is significantly less polar [22,23] as compared with the major product fractions, it is necessary to use in the mobile phase as much as 70% of MeOH (Fig. 10B). Increasing

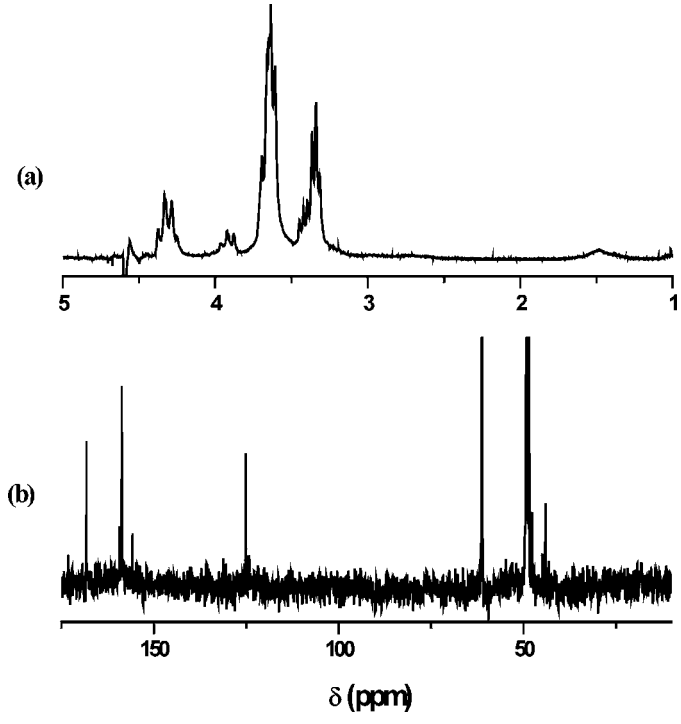

Figure 9. (a) ^{1}H-NMR and (b) ^{13}C-NMR spectra of the D_2O fraction of the products (residue) of isothermal decomposition of DIP at 305°C.

MeOH up to 90% leads to elution of pure DIP in the column dead time. On the other hand, in chromatogram in Fig. 10A, DIP is eluted at a higher MeOH percentage (DIP elution is associated with peak 12), which is probably due to the slow equilibration of mobile phase in the gradient.

CONCLUSIONS

Thermal decomposition of DIP shows a different behavior as compared with electrochemical oxidation. The TG curve, in N_2 atmosphere, presents three steps of mass loss; the first step of mass loss of around 35% of total original mass was monitored by an isothermal experiment at 305°C, the peak temperature for this change in DTG curve, producing a solid residue that upon solubilization in water gives two major products of decomposition, as detected by HPLC. Unlike in the electrochemical oxidation, the products of isothermal decomposition show an intense fluorescence shifted to lower wavelengths, suggesting a smaller reorganization of the pyrimido-pyrimidine system than that observed in the electrochemical oxidation, where

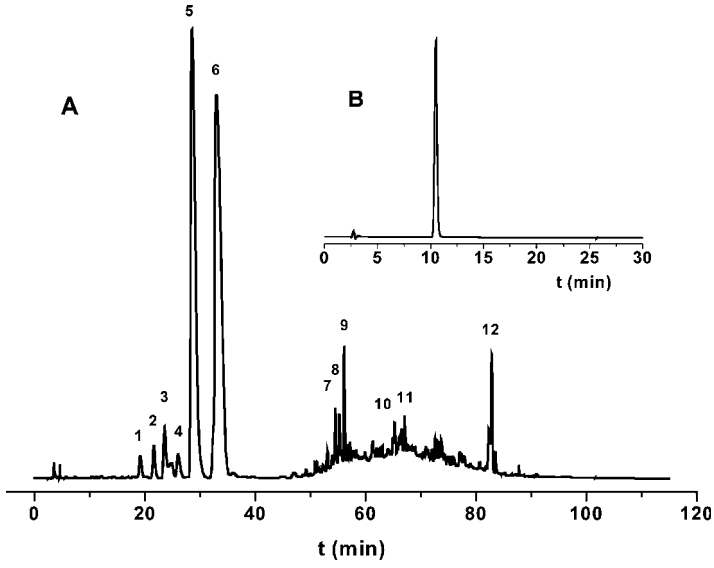

Figure 10. (A) HPLC chromatogram of the aqueous fraction of the products of isothermal decomposition of DIP. Mobile phase: mixture of acetate buffer 40 mM pH 4.0 and methanol (MeOH). Gradient: 40 min, 10% of MeOH; 40–90 min, 100% of MeOH; 90–115 min, 10% of MeOH. Stationary phase: C18, injection volume 20 1. (B) The inset shows a chromatogram for pure DIP obtained in isochratic mode in a mixture of acetate buffer 40 mM pH 4.0/MeOH (3 : 7 ratio). Retention time was 10.5 min.

the fluorescence emission disappears completely, consistent with the formation of nonfluorescent product(s). IR spectra of the lyophilized aqueous residue from isothermal treatment suggest the possibility of the presence of a carbonyl group in the product(s). NMR data suggest that the piperidine ring is absent in the products, and several methylene groups are observed. The initial loss of 35% of total mass is consistent with the dissociation of piperidine substituents. The presence of fluorescence and the observation of NMR peaks due to aromatic carbons are a strong evidence for the maintenance of the pyrimido-pyrimidine ring system and that the main changes occur in the substituent groups in positions 4 and 8. Work is in progress to characterize the two main fractions of products solubilized in aqueous solution.

ACKNOWLEDGMENTS

The authors are indebted to Brazilian agencies FAPESP and CNP_q for partial financial support. M.S.O. is a recipient of a Ph.D. grant from FAPESP.

REFERENCES

1. Steinberg, D, Workshop Participants Circulation. Antioxidants in the prevention of human artherosclerosis. *Circulation* **1992**, *85*, 2338–2344.
2. Fitzgerald, G. A. Dipyridamole. *N. Engl. J. Med.* **1987**, *316* (20), 1247–1257.
3. Batista, E.; del Prado, J.; Almirall, L.; Jamieson, G. A.; Ordinas, A. Inhibitory effects of dipyridamole on growth, nucleoside incorporation, and platelet-activating capability in the U87MG and SKNMC human tumor cell lines. *Cancer Res.* **1985**, *5* (9), 4048–4052.
4. Kang, G. J.; Kimball, A. P. Dipyridamole enhancement of toxicity to L1210 cells by deoxyadenosine and deoxycoformycin combinations in vitro. *Cancer Res.* **1984**, *44* (2), 461–466.
5. Asoh, K.; Saburi, Y.; Sato, S.; Nogae, I.; Kohno, K.; Kuwano, M. Potentiation of some anticancer agents by dipyridamole against drug-sensitive and drug-resistant cancer cell-lines. *Jpn. J. Cancer Res.* **1989**, *80* (5), 475–481.
6. Zhen, Y. S.; Taniki, T.; Weber, G. Azidothymidine and dipyridamole as biochemical response modifiers—synergism with methotrexate and 5-fluorouracil in human colon and pancreatic-carcinoma cells. *Oncology Res.* **1992**, *4* (2), 73–78.
7. Iuliano, L.; Violi, F.; Ghiselli, A.; Alessandri, C.; Balsamo, F. Dipyridamole inhibits lipid-peroxidation and scavenges oxygen radicals. *Lipids* **1989**, *24* (5), 430–433.
8. Pedulli, G. F.; Lucarini, M.; Marchesi, E.; Paolucci, F.; Roffia, S.; Fiorentini, D.; Landi, L. Medium effects on the antioxidant activity of dipyridamole. *Free Radical Biol. Med.* **1999**, *26* (3–4), 295–302.
9. Borisevitch, I. E.; Tabak, M. Electronic absorption and fluorescence spectroscopic studies of dipyridamole — effects of solution composition. *J. Lumin.* **1992**, *51* (6), 315–322.
10. Borissevitch, I. E.; Borges, C. P. F.; Borissevitch, G. P.; Yushmanov, V. E.; Louro, S. R. W.; Tabak, M. Binding and location of dipyridamole derivatives in micelles: the role of drug molecular structure and charge. *Z. Naturforsch. C Biosci.* **1996**, *51* (7–8), 578–590.
11. Borges, C. P. F.; Tabak, M. Spectroscopic studies of dipyridamole derivatives in homogeneous solutions—effects of solution composition on the electronic absorption and emission. *Spectrochim. Acta A* **1994**, *50* (6), 1047–1056.
12. Almeida, L. E.; Castilho, M.; Mazo, L. H.; Tabak, M. Voltammetric and spectroscopic studies of the oxidation of the anti-oxidant drug dipyridamole in acetonitrile and ethanol. *Anal. Chim. Acta* **1998**, *375* (3), 223–231.
13. Castilho, M.; Almeida, L. E.; Tabak, M.; Mazo, L. H. The electrochemical oxidation of the antioxidant drug dipyridamole at glassy carbon and graphite electrodes in micellar solutions. *Electrochim. Acta* **2000**, *46* (1), 67–75.
14. Berbenni, V.; Marini, A.; Bruni, G.; Maggioni, A.; Cogliati, P. Thermoanalytical and spectroscopic characterization of solid state dipyridamole. *J. Therm. Anal. Calorim.* **2002**, *68* (2), 413–422.
15. Luger, P.; Roch, J. Structure and superstructure of dipyridamole, 2,2′,2″,2‴-(4,8-dipiperidinopyrimido[5,4-d]pyrimidine-2,6diyldinitrilo)tetraethanol, $C_{24}H_{40}N_8O_4$. *Acta Crystallogr. Sect. C Cryst. Struct.* **1983**, *39*, 1454–1458.
16. Castilho, M.; Almeida, A. M. P.; Almeida, L. E.; Tabak, M.; Mazo, L. H. The electrooxidation of dipyridamole derivatives in acetonitrile solution. *J. Eletroanal. Chem.* **2002**, *528* (1–2), 175–183.
17. *The Merck Index*, Twelfth edition; Merck: Whitehouse Station, NJ, 1996.

18. Borde, B.; Cesáro, A. A DSC study of hydrated sugar alcohols. *Isomalt J. Therm. Anal. Calorim.* **2001**, *66*, 179–195.
19. Nepomuceno, M. F.; Alonso, A.; Pereira-da-Silva, L.; Tabak, M. Inhibitory effect of dipyridamole and its derivatives on lipid peroxidation in mitochondria. *Free Radic. Biol. Med.* **1997**, *23* (7), 1046–1054.
20. Borges, C. P. F.; Honda, S.; Berlinck, R. G. S.; Imasato, H.; Berci Filho, P.; Tabak, M. Synthesis, characterization and interaction with ionic micelles of tetra-acetylated dipyridamole. *Spectrochim. Acta A* **1995**, *51* (14), 2575–2584.
21. Silvernstein, R. M.; Bassler, G. C.; Morril, T. C. *Spectrometric Identification of Organic Compounds*, 5th ed.; Wiley: New York, 1991.
22. Brasileiro, A. M. P. Ph.D. thesis, Instituto de Química de São Carlos, Universidade de São Paulo: São Carlos, 2001.
23. Barberiheyob, M.; Merlin, J. L.; Pons, L.; Calco, M.; Weber, B. A. A sensitive isocratic liquid-chromatography assay for the determination of dipyridamole in plasma with electrochemical detection. *J. Liq. Chromatogr.* **1994**, *17* (8), 1837–1848.